Structure and Conformation of Bipolar Tetraether Lipid Membranes Derived from Thermoacidophilic Archaeon *Sulfolobus acidocaldarius* as Revealed by Small-Angle X-ray Scattering and High-Pressure FT-IR Spectroscopy

Parkson Lee-Gau Chong,*,† Marion Zein,‡ Tapan Kumar Khan,† and Roland Winter*,‡

Department of Biochemistry, Temple University School of Medicine, Philadelphia, Pennsylvania 19140, and Department of Chemistry, Physical Chemistry I, University of Dortmund, Otto-Hahn-Strasse 6, D-44221, Dortmund, Germany

Received: March 6, 2003; In Final Form: June 4, 2003

The phase behavior, conformation, and structure of bipolar tetraether liposomes composed of the polar lipid fraction E (PLFE) isolated from the thermoacidophilic archaeon *Sulfolobus acidocaldarius* have been studied by small-angle X-ray scattering (SAXS) and high-pressure Fourier transform infrared spectroscopy (FT-IR) at pD 2.15. The SAXS data on PLFE multilamellar vesicles in 85 wt % D_2O showed two orders of lamellar Bragg reflections over the temperature range 5−75 °C. The lamellar repeat distances *d* indicate three lamellar regions: 5−50 °C (*d*, ∼49−50 Å), 50−60 °C (∼50−54 Å), and 60−74 °C (∼54−56 Å). The 4-Å increase in *d*-spacing from 50 to 60 °C is probably due to an increase in hydration at the PLFE polar headgroups and/or a stretch of the polar headgroups toward the bulk aqueous phase. At 74−75 °C, a lamellar-to-cubic phase transition occurs. The reciprocal spacings of the cubic phases correspond to the coexistence of the inverse bicontinuous cubic phases Q_{II}^D and Q_{II}^P with lattice constants of 105 and 82 Å, respectively. At atmospheric pressure, the vibrational frequency of the CH_2 symmetric stretching mode showed transitions at ∼46−48, 61, and 74 °C, in agreement with the SAXS data. The overall 2 cm^{-1} increase in wavenumber between 61 and 74 °C indicates a transition from a rigid, gellike lipid conformation to a chain conformation with considerable disorder, as expected from cubic phases which appear above ∼74 °C. The pressure dependence (up to 15 kbar) of the symmetric CH_2 stretching vibrational wavenumber at various temperatures has also been examined. A variety of new gellike phases are observed at elevated pressures, showing again a rich polymorphism in PLFE liposomes. The most prominent pressure-induced transition involves a ∼2 cm^{-1} increase in wavenumber, which appears at 8.0 kbar at 60 °C, 8.4 kbar at 43 °C, and 10.8 kbar at 20 °C, giving an unusual negative d*T*/d*p* value. The possible source of this anomaly has been discussed in terms of the temperature attenuation of the hydrogen bond network in the polar headgroup region.

Introduction

The major component of the plasma membrane of thermoacidophilic archaeon *Sulfolobus acidocaldarius* is bipolar tetraether lipids (∼90% of the total lipids).[1−3] Among them, the polar lipid fraction E (PLFE) is a major constituent.[4] PLFE is a mixture of bipolar tetraether lipids with either a glycerol dialkylcalditol tetraether (GDNT or calditoglycerocaldarchaeol) or a glycerol dialkylglycerol tetraether (GDGT, or caldarchaeol) skeleton (Figure 1).[4−6] GDNT (∼90% of total PLFE) is linked to phospho-myo-inositol on one end and β-glucose on the other, whereas GDGT (∼10% of total PLFE) has phospho-myo-inositol attached to one glycerol and β-D-galactosyl-D-glucose to the other skeleton.[4] Both GDGT and GDNT consist of a pair of 40-carbon biphytanyl chains, with no double bonds. Each of the biphytanyl chains contains up to four cyclopentane rings, in which the number of these rings increases with increasing growth temperature.[7] In aqueous media, PLFE lipids are able to form stable multilamellar vesicles[4] as well as unilamellar liposomes of varying sizes ranging from ∼50 nm to 150 μm in diameter,[4,8,9] where PLFE lipids span the entire lamellar structure, forming a monomolecular thick membrane.[10]

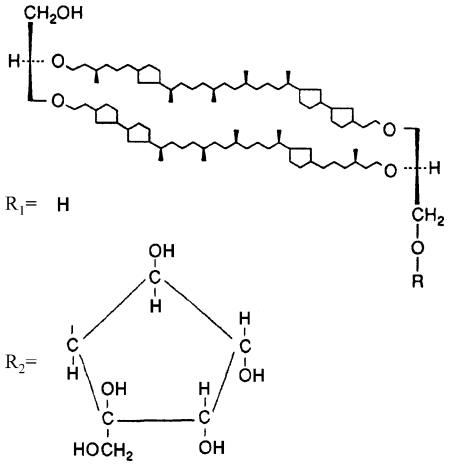

Figure 1. Structures of the GDNT (R = R_2) and GDGT (R = R_1) backbones.[6] The number of cyclopentane rings can vary from 0 to 4 in each biphytanyl chain.

PLFE liposomes have been used as a model for thermoacidophilic archaeal membranes.[6] In addition, due to their remark-

* To whom correspondence should be addressed. Dr. Roland Winter. Telephone: +49 231 755 3900. Fax: +49 231 755 3901. E-mail: winter@pci.chemie.uni-dortmund.de. Dr. Parkson Chong. Telephone: 215-707-4182. Fax: 215-707-7536. E-mail: pchong02@temple.edu.

† Temple University School of Medicine.

‡ University of Dortmund.

10.1021/jp034584d CCC: $25.00
Published on Web 07/12/2003

ably high stability against high temperature, acidic/alkaline pH, oxidation, and the actions of phospholipases, bile salts, and serum proteins, PLFE and other bipolar tetraether liposomes have been used in technological development such as sterilization,[11] immunoassays,[12] and vaccine or drug delivery.[13−16]

Previous physical studies of PLFE liposomes have focused on stability, permeation, and membrane packing. Proton permeation across PLFE liposomes was found to be low and relatively insensitive to temperature.[8,17] PLFE liposomes also exhibited unusual thermal stability in terms of dye leakage and were less permeable to the entrapped dye than nonarchaeal liposomes.[17,18] Fluorescence studies in our laboratory have further suggested that rigid membrane packing, in combination with the extensive network of hydrogen bonds in the polar headgroup regions,[19,20] contributes to the low solute permeability across PLFE liposomes, which may play a role in maintaining a large proton gradient across the plasma membrane of *S. acidocaldarius* at high growth temperatures. *S. acidocaldarius* grows at 65−85 °C and at pH 2−3, while the intracellular pH is ∼6.5.

Fluorescence studies of membrane packing in PLFE liposomes have shown a temperature-induced phase transition at 48−50 °C and the transition may involve subtle structural changes in both the polar headgroups and the hydrocarbon chains. The excitation generalized polarization (GP_{ex}) of Laurdan (2-(dimethylamino)-6-lauroylnaphthalene) fluorescence in PLFE giant unilamellar vesicles exhibited a small but distinct decrease near 50 °C, which suggests a conformational change in the PLFE polar headgroup region, where Laurdan's chromophore resides.[9] Further, the average and in-plane rotational rates of perylene in PLFE liposomes exhibited an abrupt change at ∼48 °C[21] and the lateral mobility of 1-palmitoyl-2-(10-pyrenyl)docanoyl-*sn*-glycero-3-phosphatidylcholine (PyrPC) in PLFE liposomes was highly restricted and only became appreciable at temperatures >48 °C.[22] The perylene and PyrPC results suggest that at ∼48 °C there is also a structural change in the PLFE hydrocarbon region, where perylene and the pyrene moiety of PyrPC are located.

However, fluorescence alone does not provide detailed and direct structural information about liposomes. Besides, fluorescent probes, even at a low probe-to-lipid ratio, may impose local perturbations on membrane structure.[23] To address these concerns, in this work, we have extended our studies on PLFE liposomes by using two noninvasive methods, namely, small-angle X-ray scattering (SAXS) and high-pressure Fourier transform infrared spectroscopy (FT-IR). SAXS detects changes in the long-range order of the lipid system. High-pressure FT-IR is a powerful tool to study variations in the intermolecular interactions at specified chemical bond regions, and the use of high pressure is biologically relevant as deep sea hydrothermal vent archaea live at hyperbaric conditions. Specifically, in this paper, we report the lamellar repeat distances *d*, the diffraction patterns of nonlamellar structures, and the frequencies of CH_2 vibrational bands at different temperatures or pressures. The results provide new information on the phase behavior, conformation, and structure of PLFE liposomes also at high pressure.

Experimental Approaches

Materials. *S. acidocaldarius* cells (strain DSM639, ATCC, Rockville, MD) were grown aerobically and heterotrophically at 69−70 °C, pH 2.5−3.0. PLFE lipids were isolated from *S. acidocaldarius* dry cells by Soxhlet extraction with chloroform/methanol (1:1, v/v) for 48 h, as previously described.[4] In brief, the crude lipids were fractionated by reversed-phase column chromatography using C-18 PrepSep columns eluted first with methanol:water (1:1, v/v) (filtrate A) and then with chloroform:methanol:water (0.8:2:0.8, v/v/v) (filtrate B). Filtrate B was further separated by thin-layer chromatography (TLC) (PLK5 silica gel 150A, Whatman, NJ) using a mobile phase of chloroform:methanol:water (65:25:4, v/v/v). The PLFE fraction ($R_f \approx 0.2$) was scraped from silica TLC plates and eluted with chloroform:methanol:water (1:2:0.8, v/v/v). Finally, PLFE was purified by cold methanol precipitation 2−3 times.

Sample Preparation. PLFE vesicles were prepared by codissolving the lipid in chloroform/methanol/water (65/25/10, v/v/v), vortex mixing the solution in sealed containers, and drying the solution first under a stream of nitrogen and then under vacuum for at least 16 h. The dried lipid was dissolved in D_2O, and the pD was adjusted to 2.15. D_2O was used as solvent because H_2O has overlapping IR bands with vibrational bands of lipid chains in the IR spectra. The hydrated mixture was heated in a closed vessel to a temperature of 70 °C and vortex mixed for at least 5 min to yield multilamellar vesicles.

Small-Angle X-ray Scattering. Small-angle X-ray scattering (SAXS) has been used to detect changes in the long-range order of the lipid system. The SAXS experiments were performed at beamline X13 of the EMBL outstation at DESY in Hamburg. The experimental setup has already been described in detail elsewhere.[24,25] The reciprocal spacings of the reflections of indices *hkl*, $s_{hkl} = (2/\lambda) \sin \phi$ (λ, wavelength of radiation; 2ϕ, scattering angle; $Q = 2\pi s$, momentum transfer), were calibrated in the small-angle region by the diffraction pattern of rat tail tendon collagen, and the range of scattering vectors covered is 0.05−0.25 $Å^{-1}$. No sample degradation due to radiation damage was detected. The lipid−water dispersions investigated here are equivalent to powder samples which are composed of many randomly oriented microcrystals. Thus, Bragg's condition is automatically fulfilled, and all possible diffraction peaks are simultaneously recorded. While the positions of the diffraction peaks are related to periodic distances within a lyotropic lipid mesophase, their sharpness or width reflects the extent of this periodicity over large distances. If a lipid−water phase is lacking any periodic structure, diffuse small-angle scattering is observed only. Lamellar lipid−water mesophases (denoted as L or P) consisting of alternating layers of lipid and water molecules, exhibit quasi-one-dimensional periodic structures with diffraction patterns in the small-angle regime that are described by the equation

$$s_n = n\frac{1}{d} \tag{1}$$

where $n = 1, 2, 3, \ldots$ and the lattice spacing *d* is the sum of the water and lipid layer thicknesses.

In the case of cubic lipid phases, Bragg peaks may be observed at

$$s = \frac{1}{a}\sqrt{h^2 + k^2 + l^2} \tag{2}$$

where *a* is the cubic lattice constant. The Miller indices *h*, *k*, *l* depend on the lattice type (primitive, body-centered, face-centered) and the symmetry elements of the cubic structure. In Table 1 the relative Bragg peak positions of the three most common bicontinuous cubic lipid−water phases are shown. The bicontinuous cubic phases of type II (Q_{II}) can be visualized in terms of a highly convoluted lipid layer, which subdivides three-dimensional space into two disjointed polar labyrinths separated

TABLE 1: Inverse Cubic Lipid−Water Mesophases and Expected Bragg Peak Position Ratios at Low Angles[a]

lipid−water phase	space group	peak position ratio
Q_{II}^{D}	*Pn*3*m*	$\sqrt{2}$: $\sqrt{3}$: $\sqrt{4}$:...
Q_{II}^{P}	*Im*3*m*	$\sqrt{2}$: $\sqrt{4}$: $\sqrt{6}$: ...
Q_{II}^{G}	*Ia*3*d*	$\sqrt{6}$: $\sqrt{8}$: $\sqrt{14}$: ...

[a] The cubic phases are based on lipid layers curved in three dimensions. The midplanes of the layers are D, P, or G infinite periodic minimal surfaces, as denoted with the superscripts in the phase symbols.

by an apolar septum. The structures of three of these phases, Q^{230}, Q^{224}, and Q^{229}, are closely related to the Schoen Gyroid (G), the Schwarz (D), and the Schwarz (P) infinite periodic minimal surfaces (IPMS), respectively. IPMS is an intersection-free surface periodic in three dimensions with a mean curvature that is everywhere zero.

Infrared Spectroscopy. Infrared spectra were collected on a Nicolet Magna 550 Fourier transform infrared spectrometer with a liquid-nitrogen-cooled cadmium telluride detector. The infrared beam was condensed by a spectral bench onto the diamond anvil cell. Small amounts (typically 0.04 μL) of the homogeneous PLFE dispersions resulting from the freeze−thaw cycles were then placed, together with powdered α-quartz, in the 0.5-mm diameter hole of a 0.05-mm-thick stainless steel gasket mounted on a diamond anvil cell (type IIa diamonds from Diamond Optics, Tucson, AZ), which was thermostated by an external water thermostat. Pressure was determined from the shift of the 695 cm^{-1} phonon band of α-quartz.[26] The pressure can be determined with an accuracy of ±100 bar by using this method. To achieve thermal equilibrium, a 20-min wait was adopted at each new temperature or pressure before data were taken. For each spectrum 256 interferograms were co-added, at a spectral resolution of 2 cm^{-1}, and apodized with a Happ-Genzel function. The sample chamber was purged with dry, carbon dioxide free air during data collection in order to minimize spectral contributions from atmospheric gases. All of the data analysis, including determination of the vibrational wavenumbers $\tilde{\nu}$, was done with the OMNIC software developed by Nicolet Instruments.

Fourier transform infrared spectroscopy has been shown to be a valuable tool for studying the phase behavior and the conformation of lipid membrane systems. The most sensitive vibrational modes in the infrared spectra of phospholipids to monitor phase transitions are the stretching or bending vibrations of methylene groups. Analysis of the symmetric and antisymmetric stretching modes of the methylene chains, which are located in the spectral region between 2800 and 3000 cm^{-1}, yields information about conformational rearrangements of the chains and thus allows detection of transformations between phases that differ in acyl chain packing and conformation.[27,28] Besides temperature-dependent studies, pressure-dependent studies can be performed using diamond-anvil cells. Applying pressure in the 15-kbar regime only affects the intermolecular distances and, unlike temperature, does not impart thermal energy to the system. Therefore changes in the infrared spectrum of the lipid system can be directly related to variations in the intermolecular interactions, which can be caused by bond strengthening or weakening, conformational changes, or hydration effects at the polar/apolar interface. In general, higher pressure decreases the intermolecular distances and increases the repulsion forces between the atoms, leading to a linear increase of the stretching vibrations. Deviations from this linear pressure dependence can be interpreted in terms of phase transformations in connection with structural or conformational changes of the lipid system. However, in multicomponent lipid membranes, as in PLFE liposomes, curved lines are also possible, especially when passing two-phase coexistence regions; in this case, a sudden discontinuity in stretching vibrations may be considered as a phase transition.

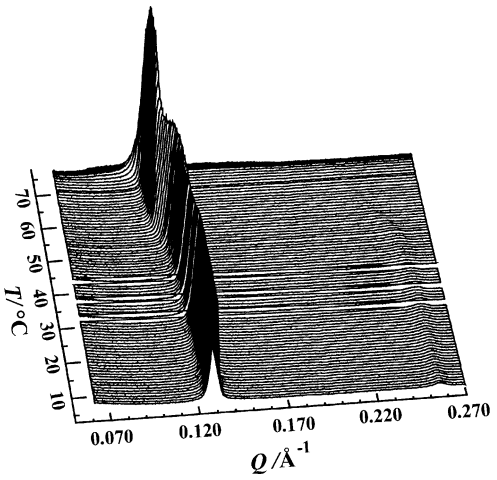

Figure 2. Small-angle X-ray pattern of PLFE in excess water (85 wt % D_2O) at pD 2.15.

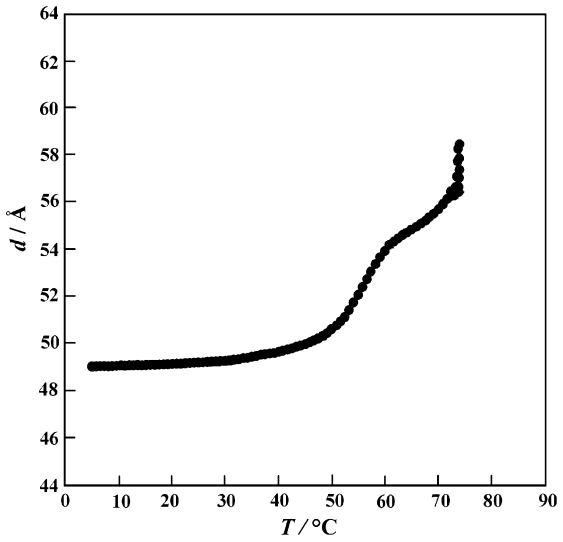

Figure 3. Lamellar repeat unit *d* of PLFE in excess water (85 wt % D_2O) as a function of temperature.

Results and Discussion

SAXS. Figure 2 shows the SAXS data on PLFE multilamellar vesicles in 85 wt % D_2O at pD 2.15. The temperature range covered was from 5 to 75 °C. As can be clearly seen, two orders of lamellar Bragg reflections are visible over this temperature range. The lamellar repeat distances *d* calculated from the Bragg equation are shown in Figure 3. The structures observed between 5 and 74 °C may be attributed to three lamellar phase regions with different temperature dependencies of their lamellar lattice constant. These regions are 5−50 °C (denoted L_1), 50−60 °C (L_2), and 60−74 °C (L_3). The *d*-spacing is ∼49−50 Å up to 50 °C with a small (1 Å) increase above 35 °C. Then, *d* increases linearly up to 54 Å at 60 °C, followed by a slight increase up to 74 °C. The changes observed in *d*-spacing as a function of temperature in the range 5−74 °C can be due to changes in the tilt angle of the lipid molecules with respect to the lipid layer normal, in the degree of hydration at the polar headgroups, and/or in the lateral and transverse rearrangement of the lipid

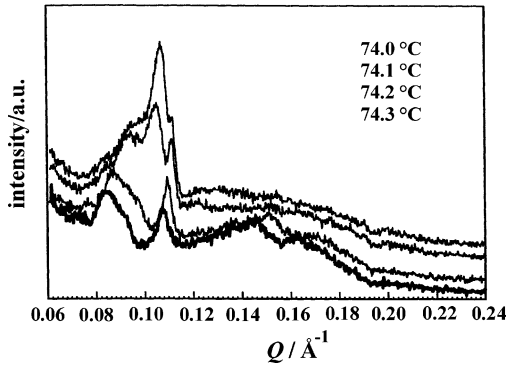

Figure 4. Small-angle X-ray pattern of PLFE in excess water above 74 °C (85 wt % D_2O; scan rate 1 deg/min).

components, which can be accompanied by changes in lipid conformation.

Above 74 °C, a major phase transformation occurs (Figure 3), indicated by a slow change in the diffraction pattern with time. As the lipid system consists of a complex mixture of GDGT and GDNT lipid molecules, no pure one-phase regions and hence no sharp transformations between phases might be expected. Instead, more or less broad phase coexistence regions are envisaged. A blow-up of the diffraction patterns above 74 °C is shown in Figure 4. The diffraction patterns indicate the transition from lamellar to nonlamellar structures. The diffraction data between 74.0 and 74.3 °C are in agreement with a phase coexistence region between diminishing lamellar and developing nonlamellar phases of cubic symmetry. Although the assignment of the diffraction peaks to mesophase structures is difficult with these few and broad peaks, the reciprocal spacings of the new phases can tentatively be assigned to two coexisting bicontinuous cubic phases. Besides the weak reflection of the remaining lamellar phase around 0.093 $Å^{-1}$, the diffraction pattern at 74.3 °C exhibits additional reflections at about 0.073, 0.084, 0.108, and 0.146 $Å^{-1}$, which can tentatively be indexed assuming a coexistence of the inverse bicontinuous cubic structures Q_{II}^D and Q_{II}^P with lattice constants of 105 and 82 Å, respectively. The rather broad Bragg reflections are due to the lack of long-range order. Interestingly, the ratio of the lattice constants of the cubic structures Q_{II}^D and Q_{II}^P, $a(Q_{II}^D)/a(Q_{II}^P)$, is 1.28, which is indeed what is expected theoretically (1.279) for these two bicontinuous cubic structures being in equilibrium with each other in excess water, and thus supports the tentative peak assignment. The data are too scanty to justify a more detailed analysis here, however.

Cubic phases Q_{II}^D and Q_{II}^G (rather than Q_{II}^P) have previously been detected in the total polar lipid extract (PLE) from the plasma membrane of *Sulfolobus solfatarius*, a thermoacidophilic archaeon with lipid compositions resembling those in *S. acidocaldarius*.[29] In addition, Q_{II}^G was detected in the PL fraction[30] and in the hydrolyzed GDNT lipids[29] of the PLE from *S. solfataricus*. However, in the studies of Gulik et al.[29,30] no cubic phase was reported for the P2 lipid fraction from *S. solfataricus*, which is similar to the PLFE lipid fraction from *S. acidocaldarius* with regard to lipid composition. This discrepancy may be attributed to the differences in experimental conditions (e.g., pH and water content) and/or to subtle differences in lipid composition. Note that, at a given growth temperature, the number of cyclopentane ring in tetraether lipids has a broad range, rather than a fixed value.[6,16,31] The average number and the distribution of the ring may vary with growth conditions in a species-dependent manner.

Due to the limited PLFE lipids isolated, no wide-angle X-ray scattering (WAXS) was measured in this study. However, as

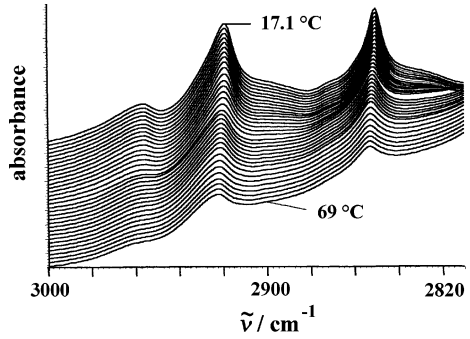

Figure 5. Temperature dependence of the IR spectra of PLFE in D_2O in the CH_2 symmetric and antisymmetric stretching mode region at pD 2.15.

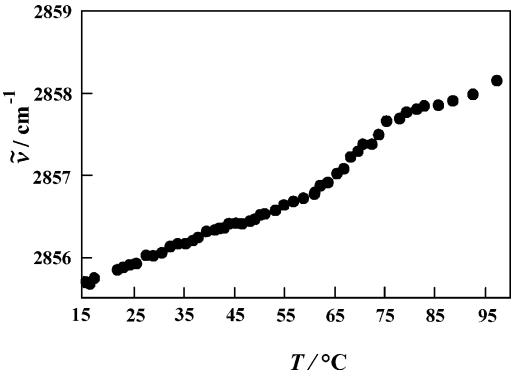

Figure 6. Effect of temperature on the wavenumber of the symmetric CH_2 stretching mode of PLFE in D_2O.

PLFE consists of a complex lipid mixture (GDNT and GDGT with varying numbers of cyclopentane rings in the hydrocarbon chain) with heterogeneous lateral lipid organization over large regions of the phase field, we do not expect the WAXS data to yield clear-cut information.

Temperature- and Pressure-Dependent FT-IR Spectroscopy. To yield further information on the conformational changes and phase behavior of PLFE dispersions in excess water, FT-IR measurements were performed. Temperature-dependent measurements were performed in the range 5−100 °C and spectra were taken in steps of about 1 deg. Figure 5 shows the infrared spectra of PLFE dispersions in the wavenumber region from 3000 to 2800 cm^{-1} at different temperatures. Absorption bands at ∼2855 and 2923 cm^{-1} are assigned to CH_2 symmetric and antisymmetric stretching vibrations of PLFE, respectively. The absorption bands in PLFE are much broader in contrast to those of monopolar diester phospholipids,[28] which might be due to overlapping bands of the lipid components GDNT and GDGT. The biphytanyl chains of PLFE contain also branched methyl groups and cyclopentane rings; but their absorption bands could not be detected with sufficient accuracy due to their low concentrations and/or low transition dipole moments.

Figure 6 shows the temperature dependence of the symmetric CH_2 stretching vibration of PLFE. The wavenumber of the symmetric stretching vibration is a measure of the conformational disorder of the lipid chains. For example, in monopolar diester phospholipid bilayers, an increase of about 2 cm^{-1} is observed when passing the $L_{\beta'}-L_\alpha$ gel-to-fluid transition, which is accompanied by a significant increase in conformational disorder, i.e., an increase in the number of gauche conformers and kinks.[28] In Figure 6, transitions are evident at ∼46−48, 61, and 74 °C, in reasonable agreement with the phase boundaries derived from the SAXS data (Figure 3).

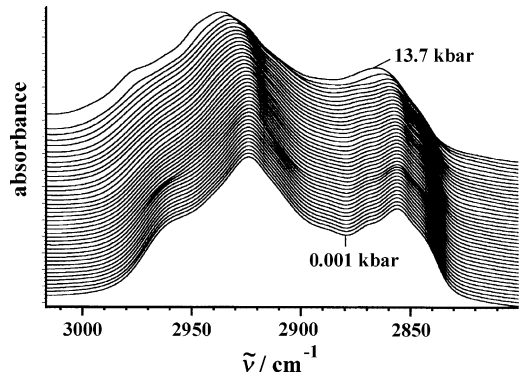

Figure 7. Pressure contours of the CH_2 stretching vibrations of PLFE in D_2O at $T = 20$ °C.

The significant increase in vibrational wavenumber at 46−48 °C indicates a transition from a rigid-gel-type structure (probably $L_{\beta'}$- or L_β-like) to another lamellar gel phase with increased conformational disorder of the lipid chains. The overall 2 cm^{-1} increase in wavenumber between 61 and 74 °C (Figure 6) indicates that a transition from a rigid, gellike lipid conformation to a chain conformation with considerable conformational disorder is reached at 74 °C, which is indeed expected when fluidlike cubic structures are formed. The structure between 61 and 74 °C could be a fluidlike lamellar structure of type L_α. The transition at ∼46−48 °C detected by FT-IR (Figure 6) agrees with not only the transition at ∼50 °C revealed by SAXS (Figure 3) but also the fluorescence data obtained from Laurdan,[9] perylene,[21] and PyrPC,[22] as mentioned earlier. The transitions at 61 and 74 °C reported in this study (Figures 3 and 6) are new findings; they were not detected in previous fluorescence studies, probably due to the large temperature increments and the limited tempreature range employed.[9,21]

Figure 7 shows the pressure dependence of the CH_2 symmetric and antisymmetric stretching mode region at 20 °C. The data were taken isothermally at various pressures up to ∼15 kbar. The maximum of the symmetric CH_2 stretching vibrational wavenumber as a function of pressure at four selected temperatures is presented in Figure 8a−d. In these plots, break points visible in the data would suggest pressure-induced phase transition points at the temperature chosen. For example, at 13 °C (Figure 8a), a new pressure-induced phase (L4) appears around 0.8 kbar, which is probably a further lamellar gel phase, as an increase in pressure requires a reduction in partial molar lipid volume, which is best accommodated in a solidlike lamellar state. This interpretation is supported by the linear increase of wavenumber with pressure beyond 0.8 kbar (Figure 8a). As shown in previous studies on pure monopolar diester phospholipid membranes, due to increased repulsive interactions, an increase in the methylene stretching frequency with increasing pressure is observed when the lipid is in the ordered gel state.[28,32]

The plots in Figure 8b−d (at 20, 43, and 60 °C) also showed an increase in wavenumber with increasing pressure, but the increase is not always linear. Thus it is rather difficult to identify all the possible break points unambiguously. Nevertheless, the data in Figures 8b−d reveal two important points. First, there exists a rather complex phase behavior for PLFE membranes under pressure. For example, at 20 °C, pressure-induced phase transitions seem to occur at around 2.0, 3.2, 5.4, and 10.8 kbar. This result shows that PLFE liposomes are similar in complexity to pure monopolar diester phospholipid bilayers such as dipalmitoylphosphatidylcholine in excess water, which exhibits 5 gel phases up to pressures of 15 kbar.[25,33]

Second, each plot exhibits a dramatic (∼2 cm^{-1}) increase in wavenumber at a specific pressure, namely, 8.0 kbar at 60 °C (Figure 8d), 8.4 kbar at 43 °C (Figure 8c), and 10.8 kbar at 20 °C (Figure 8b). These sharp increases in wavenumber can be easily interpreted as a phase transition to an even more ordered state. Interestingly, the critical pressure for the sharp transition increases with decreasing temperature. This temperature dependence of the transition pressure is rather unusual because the critical pressure of a disordering-ordering lipid phase

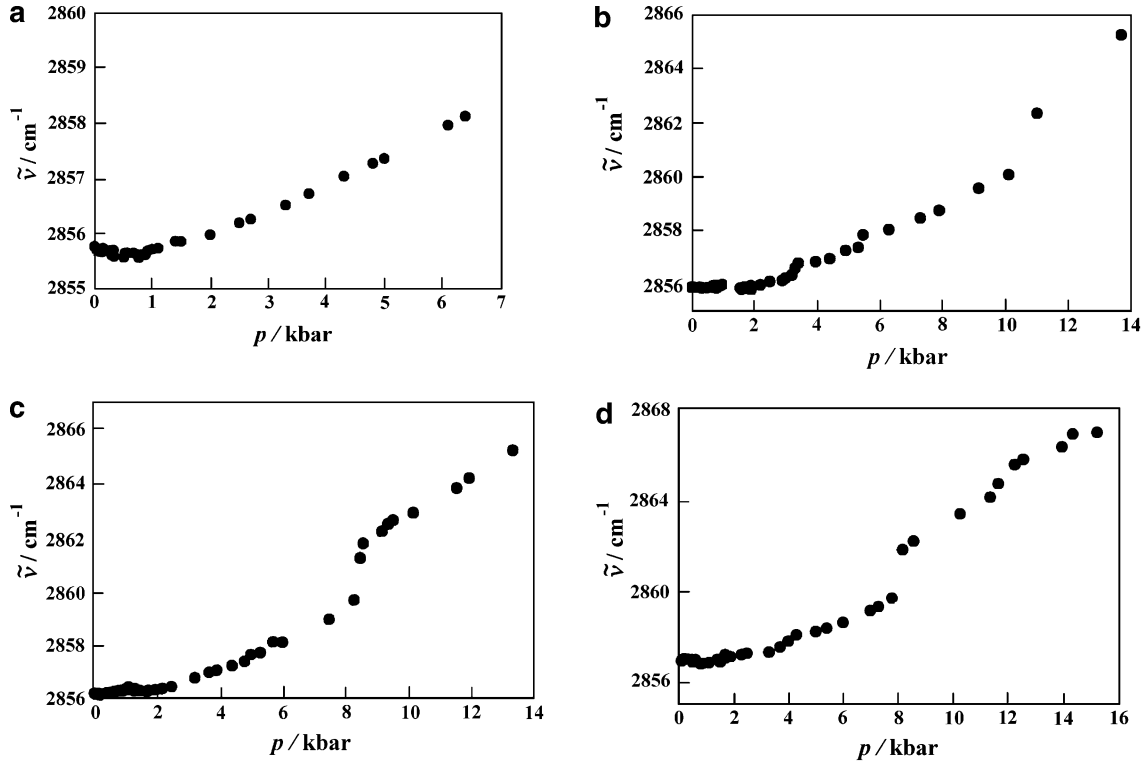

Figure 8. Pressure dependence of the CH_2 symmetric stretching mode wavenumber of PLFE in D_2O at (a) 13, (b) 20, (c) 43, and (d) 60 °C.

transition usually increases with increasing temperature, generating a positive dT/dp value.[34−37]

The negative dT/dp value for the sharp transition seen in Figures 8b−d may be understood as follows. In the polar headgroup regions of bipolar tetraether liposomes, there is an extensive network of hydrogen bonds between the sugar residues exposed at the outer surface of the membrane.[17,19,20] Increased temperature would attenuate the hydrogen bond network in the polar headgroup region, which might facilitate certain conformational changes in the biphytanyl chain region. As a result, less pressure is needed to reduce the membrane free volume in the biphytanyl chain region in order to reach a more ordered physical state that corresponds to the sharp pressure-induced phase transition shown in Figure 8b−d.

Comparison with Previous Fluorescence Studies. Previous fluorescence studies on PLFE liposomes showed one phase transition at ∼48−50 °C.[9,21,22] The present IR and SAXS data not only confirm the existence of this phase transition but also help to delineate the conformational changes of PLFE lipids associated with this transition. In a microscopy study, we have shown that the average excitation generalized polarization (GP) of Laurdan fluorescence in the center cross section of PLFE giant unilamellar vesicles (GUVs) at pH 2.86 exhibits an abrupt change at ∼50 °C.[9] Below 50 °C, the GP values are slightly below zero and relatively invariant with temperature; however, from 50 to 65 °C, Laurdan's GP decreases sharply with incresing temperature, reaching −0.24 at 65 °C. It is well established that Laurdan's GP decreases with increasing local polarity. Thus, a lower GP value above 50 °C indicates that through this phase transition Laurdan experiences more solvent relaxation due to increased interactions with water or neighboring lipid polar headgroups. Since Laurdan's chromophore resides in the polar headgroup region,[9] the abrupt change in Laurdan's GP at 50 °C[9] is most likely due to a temperature-induced stretching of the polar headgroup toward the bulk solution. This stretching may originate from the thermal attenuation of the hydrogen bond network between the sugar moieties of the polar headgroups. Perhaps as a result of this stretching and the accompanied increase in hydration, the *d*-spacing is increased by ∼4 Å from 50 to 60 °C (Figure 3) and solvent relaxation is increased as well.[9]

The idea that the phase transition at ∼48−50 °C is mainly due to the stretching of the polar headgroups of PLFE, rather than a gross stretching in the hydrocarbon region, is consistent with the magnitude of the change in Laurdan's GP through this transition. At ∼50 °C, the excitation GP of Laurdan fluorescence in PLFE GUVs exhibits a distinct but small change, i.e., from ∼0 to −0.1 at pH 2.6.[9] In contrast, the main gel-to-liquid crystalline phase transition in saturated monopolar diester liposomes leads to a large change in GP, for example, from 0.6 to −0.2 in the case of dipalmitoylphosphatidylcholine bilayers.[38] This small change in PLFE structure agrees with the differential scanning claorimetric scans, which showed no or little enthalpy changes (communications with Dr. E. Chang).

An increase in *d*-spacing for a lipid phase transition from a rigid gel-type structure to another lamellar gel phase with increased conformational disorder (discussed earlier) is explainable. In some monopolar diester liposomes, the main ordering−disordering phase transition results in a decrease in *d*-spacing[39] because of the structural change from an extended all-trans configuration in the polymethylene chain to a flexible one containing gauche conformations. The structure of the hydrocarbon chains in monopolar diester lipids is very different from that in PLFE. Each of the two biphytanyl chains of PLFE contains branched methyl groups and cyclopentane rings, and each biphytanyl chain is covalently linked from one polar end to the other. Such a rigid hydrocarbon chain does not possess an excessive trans-to-gauche conformational transition normally seen in the acyl chains of monopolar diester phospholipids. Thus, the thickness of the hydrocarbon region of PLFE liposomes is expected to change relatively little through the ordering−disordering transition. This point argues for the idea that the increased *d*-spacing from 50 to 60 °C (Figure 3) mainly comes from the stretching of the PLFE polar headgroups, rather than the stretching of the hydrocarbon regions. This argument is supported by the study of the synthetic bipolar tetraether lipid 1,1′-*O*-eicosamethylene-2,2′-di-*O*-decyl-*rac*-diglycero-3,3′-diphosphate, which lacks cyclopentane rings and branched methyl groups, has only one polymethylene chain covalently linked from one polar end to the other, and has phosphate as the sole polar headgroup.[40] Without a high molecular rigidity in the hydrcarbon regions and a sufficient length in the polar headgroup regions, the interlamellar spacing of this synthetic bipolar tetraether lipid showed a sharp 8-Å decrease, rather than an increase, from below 47 °C to above.[40]

The aforementioned phase behavior and the lipid conformation in the neighborhood of ∼48−50 °C appear to be important in governing PLFE membrane properties. First, the lateral mobility of PyrPC in PLFE multilamellar vesicles (MLVs) is minimal until 48 °C,[22] a result later confirmed by a ^{31}P NMR study on tetraether liposomes from *Thermoplasma acidophilum*, a thermoacidophilic archaeon grown at pH 2 and 55−59 °C.[41] Second, there is an abrupt increase in perylene rotational rates in PLFE MLVs at 48 °C.[21] These two fluorescent probe studies suggest that PLFE MLVs are rigid and tightly packed at low temperatures, but they begin to gain appreciable "membrane fluidity" at temperatures higher than 48 °C. Third, proton permeation across PLFE unilamellar vesicles seems to undergo a rather dramatic increase at temperatures above 49−52 °C (Figures 6B and 7A in ref 21).

In addition to the 48−50 °C phase transition, our previous microscopy study shows the formation of stable domains in the Laurdan fluorescence intensity images of PLFE GUVs at pH 2.68 below 20−24 °C.[9] Those domains have been attributed to lipid lateral separation,[9] rather than lipid conformational changes. This explanation is consistent with our present SAXS and IR data, which do not show any appreciable change in *d*-spacing and CH_2 stretchings in the neighborhood of 20−24 °C. The domains seen in Laurdan fluorescence images do not move significantly in the plane of the membrane,[9] which suggests that PLFE liposomes are rigid and tightly packed, so little free volume is available for lateral diffusion at these low temperatures. A similar conclusion was derived from PyrPC fluorescence studies.[22] Despite the tight and rigid packing for the movement of bulky fluorescent probes, our present IR data show that the biphytanyl chains of PLFE have sufficient local free volume for CH_2 stretching as this vibration is sensitive to pressure (Figure 8). Indeed, molecular modeling has displayed some deadspace between PLFE biphytanyl chains.[41]

Concluding Remarks. Due to the low yield in PLFE lipid isolation and purification, we do not have sufficient amounts of lipids to construct a phase diagram, which would require separation of GDNT and GDGT from PLFE, and to test the metastability of the obtained phases. The phase transitions observed here are not compared with those obtained from hydrolytic GDNT and hydrolytic GDGT,[42] which do not have the sugar moieties, a crucial part for the unique structural properties of bipolar tetraether lipids. Nevertheless, our present

data show that, as with many monopolar diester phospholipid bilayers, PLFE bipolar tetraether liposomes exhibit a rich polymorphism, which might reflect a fundamental property of archaeal lipids closely related to their physiological role. The cubic phase near 74 °C could have an important physiological meaning. It is possible that near the physiological temperature (69−70 °C in this study) the cell needs some nonlamellar spots in the plasma membrane for cell division or endocytosis. Interestingly, in a similar organism, *S. solfataricus*, a cubic phase was found in liposomes composed of the total lipid extract also at about 74 °C.[29,30] In the present study, a remarkable number and variety of phases are observed over a temperature range close to physiological conditions, and further phases have been observed at elevated pressures. The latter may bear some biological relevance as thermoacidophilic archaea live also at deep sea hydrothermal vents. Owing to the complex lipid mixture, all phases may not be strongly homogeneous. Between the low-temperature (50 °C) gellike and high-temperature (61 °C) fluidlike phase, a phase coexistence region may be envisaged, according to the Gibbs phase rule. Such a phase coexistence region of fluidlike and gellike domains does not exhibit sharp phase boundaries but rather exhibits more smooth transition curves, leading to the more gradual and continuous changes observed. Apparently, the presence of branched methyl groups, cyclopentane rings, ether linkages, and membrane spanning structures is compatible with the formation of a variety of lamellar phases with solidlike stiff chains and high packing density. Fluidization of these lipid chains gives way to the formation of cubic phases with different symmetry and topology. Both lamellar and cubic phases may find applications. PLFE lamellar vesicles have unusually high thermal, chemical, and mechanical stability; thus, they, especially when mixing with "normal" lipids, are suitable for drug delivery. For this purpose, the vesicles must be highly stable in the circulation but not too stiff to release entrapped drugs. In this regard, the PLFE lamellar phase at 50−60 °C may be most valuable. Future studies of PLFE cubic phases under various experimental conditions may find applications in membrane-protein crystallization.[43−45]

Acknowledgment. We are grateful to the Deutsche Forschungsgemeinschaft and the Fonds der Chemischen Industrie (to R.W.) and to the NSF Grant MCB-9513669 and the US Army Research Office Grant DAAD19-02-1-0077 (to P. L.-G. C.).

References and Notes

(1) Langworthy, T. A.; Pond, J. L. In *Thermophiles: General, Molecular, and Applied Microbiology*; Brock, T. D., Ed.; John Wiley & Sons: New York, 1986; pp 107−134.

(2) De Rosa, M.; Gambacorta, A.; Gliozzi, A. *Microbiol. Rev.* **1986**, *50*, 70−80.

(3) Kates, M. in *The Archaebacteria: Biochemistry and Biotechnology*; Danson, M. J., Hough, D. W., Lunt, G. G., Eds.; Portland Press: London, 1992; pp 51−72.

(4) Lo, S.-L.; Chang, E. L. *Biochem. Biophys. Res. Commun.* **1990**, *167*, 238−243.

(5) Sugai, A.; Sakuma, R.; Fukuda, I.; Kurosawa, N.; Itoh, Y. H.; Kon, K.; Ando, S.; Itoh, T. *Lipids* **1995**, *30*, 339−344.

(6) Gliozzi, A.; Relini, A.; Chong, P. L.-G. *J. Membr. Sci.* **2002**, *206*, 131−147.

(7) De Rosa, M.; Esposito, E.; Gambacorta, A.; Nicholaus, B.; Bu'lock, J. D. *Phytochemistry* **1980**, *19*, 827−831.

(8) Komatsu, H.; Chong. P. L.-G. *Biochemistry* **1998**, *37*, 107−115.

(9) Bagatolli, L.; Gratton, E.; Khan, T. K.; Chong, P. L.-G. *Biophys. J.* **2000**, *79*, 416−425.

(10) Elferink, M. G. L.; de Wit, J. G.; Demel, R.; Driessen, A. J. M.; Konings, W. N. *J. Biol. Chem.* **1992**, *267*, 1375−1381.

(11) Choquet, C. G.; Patel, G. B.; Beveridge, T. J.; Sprott, G. D. *Appl. Microbiol. Biotechnol.* **1994**, *42*, 375−384.

(12) Tomioka, K.; Kii, F.; Fukuda, H.; Katoh, S. *J. Immunol. Methods* **1994**, *176*, 1−7.

(13) Freisleben, H.-J.; Bormann, J.; Litzinger, D. C.; Lehr, F.; Rudolph, P.; Schatton, M.; Huang, L. *J. Liposome Res.* **1995**, *5*, 215−223.

(14) Krishnan, L.; Dicaire, C. J.; Patel, G. B.; Sprott, G. D. *Infect. Immun.* **2000**, *68*, 54−63.

(15) Patel, G. B.; Sprott, G. D. *Crit. Rev. Biotechnol.* **1999**, *19*, 317−357.

(16) Gliozzi, A.; Relini, A. In *Handbook of Nonmedical Applications of Liposomes*; Barenholz, Y., Lasic, D. D., Eds.; CRC Press: Boca Raton, FL, 1996; Vol. II., pp 329−348.

(17) Elferink, M. G. L.; de Wit, J. G.; Driessen, A. J. M.; Konings, W. N. *Biochim. Biophys. Acta* **1994**, *1193*, 247−254.

(18) Chang, E. L. *Biochem. Biophys. Res. Commun.* **1994**, *202*, 673−679.

(19) Elferink, M. G. L.; de Wit, J. G.; Driessen, A. J. M.; Konings, W. N. *Eur. J. Biochem.* **1993**, *214*, 917−925.

(20) Vilalta, I.; Gliozzi, A.; Prats, M. *Eur. J. Biochem.* **1996**, *240*, 181−185.

(21) Khan, T. K.; Chong, P. L.-G. *Biophys. J.* **2000**, *78*, 1390−1399.

(22) Kao, Y. L.; Chang, E. L.; Chong, P. L.-G. *Biochem. Biophys. Res. Commun.* **1992**, *188*, 1241−1246.

(23) Chong, P. L.-G.; Capes, S.; Wong, P. T. T. *Biochemistry* **1989**, *28*, 8358−8363.

(24) Czeslik, C.; Malessa, R.; Winter, R.; Rapp, G. *Nucl. Instrum. Methods Phys. Res., Sect. A* **1996**, *368*, 847−851.

(25) Czeslik, C.; Reis, O.; Winter, R.; Rapp, G. *Chem. Phys. Lipids* **1998**, *91*, 135−144.

(26) Wong, P. T. T.; Moffatt, D. J.; Baudais, F. L. *Appl. Spectrosc.* **1985**, *39*, 733−735.

(27) Wong, P. T. T.; Siminovitch, D. J.; Mantsch, H. H. *Biochim. Biophys. Acta* **1988**, *47*, 139−171.

(28) Reis, O.; Winter, R.; Zerda, T. W. *Biochim. Biophys. Acta* **1996**, *1279*, 5−16.

(29) Gulik, A.; Luzzati, V.; de Rosa, M.; Gambacorta, A. *J. Mol. Biol.* **1985**, *182*, 131−149.

(30) Gulik, A.; Luzzati, V.; de Rosa, M.; Gambacorta, A. *J. Mol. Biol.* **1988**, *201*, 429−435.

(31) De Rosa, M.; Gambacorta, A. *Prog. Lipid Res.* **1988**, *27*, 153−175.

(32) Chong, P. L.-G.; Wong, P. T. T. *Biochim. Biophys. Acta* **1993**, *1149*, 260−266.

(33) Wong, P. T. T.; Mantsch, H. H. *J. Chem. Phys.* **1985**, *83*, 3268−3274.

(34) Liu, N. I.; Kay, R. L. *Biochemistry* **1977**, *16*, 3484−3486.

(35) Chong, P. L.-G.; Weber, G. *Biochemistry* **1983**, *22*, 5544−5550.

(36) Mountcastle, D. B.; Biltonen, R. L.; Halsey, M. J. *Proc. Natl. Acad. Sci. U. S. A.* **1978**, *75*, 4906−4910.

(37) Srinivasan, K. R.; Kay, R. L.; Nagle, J. F. *Biochemistry* **1974**, *13*, 3494−3496.

(38) Parasassi, T.; De Stasio, G.; d'Ubaldo, A.; Gratton, E. *Biophys. J.* **1990**, *57*, 1179−1186.

(39) Winter, R.; Landwehr, S.; Brauns, T.; Erbes, J.; Czeslik, C.; Reis, O. In *High-Pressure Effects in Molecular Biophysics and Enzymology*; Markley, J. L., Northrop, D. B., Royer, C. A., Eds.; Oxford University Press: New York, 1996; pp 274−297.

(40) Thompson, D. H.; Wong, K. F.; Humphry-Baker, R.; Wheeler, J. J.; Kim, J.-M.; Rananavare, S. B. *J. Am. Chem. Soc.* **1992**, *114*, 9035−9042.

(41) Gabriel, J. L.; Chong, P. L.-G. *Chem. Phys. Lipids* **2000**, *105*, 193−200.

(42) Bruno, S.; Cannistraro, S.; Gliozzi, A.; De Rosa, M.; Gambacorta, A. *Eur. Biophys. J.* **1985**, *13*, 67−76.

(43) Chiu, M. L.; Nollert, P.; Loewen, M. C.; Belrhali, H.; Pebay-Peyroula, E.; Rosenbusch, J. P.; Landau, E. M. *Acta Crystallogr., Sect. D* **2000**, *56*, 781−784.

(44) Gouaux, E. *Structure* **1998**, *6*, 5−10.

(45) Nollert, P.; Royant, A.; Pebay-Peyroula, E.; Landau, E. M. *FEBS Lett.* **1999**, *457*, 205−208.